

# On the possible role of condensation-related hydrostatic pressure adjustments in intensification and weakening of tropical cyclones

Anastassia M. Makarieva<sup>1,2</sup> and Andrei V. Nefiodov<sup>1</sup>

<sup>1</sup>Theoretical Physics Division, Petersburg Nuclear Physics Institute, Gatchina 188300, St. Petersburg, Russia

<sup>2</sup>Institute for Advanced Study, Technical University of Munich, Lichtenbergstrasse 2 a, D-85748 Garching, Germany

**Correspondence:** A. M. Makarieva (ammakarieva@gmail.com)

**Abstract.** It is shown that condensation and precipitation do not disturb the hydrostatic equilibrium if the local pressure sink (condensation rate expressed in pressure units) is proportional to the local pressure, with a proportionality coefficient  $k$  that is independent of altitude. In the real atmosphere, condensation rate is controlled, among other factors, by the vertical velocity that can vary freely over height. This means that, in general, condensation disturbs hydrostatic equilibrium and thus causes pressure adjustments through redistribution of air masses. It is proposed that  $k$  maximised in the upper atmosphere results in additional upward motion, which leads to cyclone strengthening. Conversely,  $k$  maximised closer to the surface produces additional downward motion, which causes cyclone's weakening. The maximum scale of both effects should be set by the strength of the mass sink (precipitation). Using observational data, it is found that the mean intensification and weakening rates (8 and 6 hPa day<sup>-1</sup>, respectively) in Atlantic tropical cyclones constitute about two thirds of their maximum concurrent precipitation (multiplied by gravity). This means that the storms intensify at *positive* vertically integrated air convergence – a pattern impossible in modeled dry hurricanes – with the pressure tendency being negative solely due to the fact that precipitation exceeds the vertically integrated moisture convergence by absolute magnitude. The implications of these results for recent studies evaluating the (de-)intensification process based on a mass continuity equation that neglects the mass sink are discussed.

## 1 Introduction

The drop in central surface pressure is a key parameter of tropical cyclones, closely linked to their intensity (i.e., maximum wind velocity). Historically, theoretical research on storm intensification has focused primarily on describing changes in maximum velocity (Montgomery and Smith, 2017). Sparks and Toumi (2022a) made a notable effort to explain the physics of storm intensification by examining the surface pressure tendency.

In a hydrostatic atmosphere, surface pressure reflects the weight of the atmospheric column. Consequently, the surface pressure tendency indicates changes in that column's mass. According to the law of mass conservation, the rate of change of air mass in the column is equal to the vertically integrated air convergence plus evaporation  $E$  minus precipitation  $P$ . This leads to the following equation for surface pressure tendency:

$$\frac{\partial p}{\partial t} = -g \int_0^H \text{div}(\rho \mathbf{u}) dz + g(E - P), \quad (1)$$

as derived, for example, in Trenberth (1991, Eq. (5)) and Wacker et al. (2006, Eq. (23)). Here,  $p$  is surface pressure,  $g$  is the acceleration of gravity,  $\rho$  is the mass density of air,  $\mathbf{u}$  is the horizontal velocity, and  $H$  is a height at which  $\rho$  can be assumed negligible,

Assuming approximate axial symmetry of tropical cyclones, the relevant quantity becomes the mean surface pressure tendency within a cylinder of radius  $r$ , which can be expressed using Eq. (1) as:

$$\frac{\partial \bar{p}}{\partial t} = -\frac{2g}{r} \int_0^H \rho u_r dz - g\bar{P}, \quad (2)$$

as in Eq. (6) of Lackmann and Yablonsky (2004). Here,  $u_r$  denotes the radial velocity, and the averaging is performed over the cylinder's area. Evaporation is neglected, as it is generally small in the storm core (see, e.g., Makarieva et al., 2017, their Table1).

Lackmann and Yablonsky (2004), using a numerical model, found that during the intensification phase of Hurricane Lili (2002), the average pressure drop within a  $r = 100$  km radius from the storm center was approximately  $\partial \bar{p} / \partial t = -0.5$  hPa/hour. At the same time, the average pressure-equivalent mass loss from precipitation was three times greater:  $-g\bar{P} = -1.5$  hPa/hour. This led Lackmann and Yablonsky (2004) to conclude that “the amount of atmospheric mass removed via precipitation exceeded that needed to explain the model sea level pressure decrease”.

In the case of Hurricane Lili (2002), where

$$-g\bar{P} = k \frac{\partial \bar{p}}{\partial t} \quad (3)$$

with  $k \sim 3$ , omitting the precipitation term from the pressure tendency equation (2) and diagnosing pressure change solely from the air convergence term (the first term on the right-hand side of Eq. (2)) would result in a substantial error: the predicted pressure tendency would not only be twice as large in absolute

magnitude as the observed value but also incorrect in sign (positive). In other words, neglecting precipitation would suggest a rapidly weakening storm instead of a rapidly intensifying one.

We emphasize that  $k > 1$  in Eq. (3) implies that the storm intensifies with a *positive vertically integrated air convergence* (i.e., more air flows laterally into the cylinder than out). This stands in fundamental contrast to dry circulations, where a surface pressure drop can occur only if the vertically integrated air convergence is negative.

Wacker et al. (2006) reported a similar pattern in a modeled cyclone that deepened by about 60 hPa over 90 hours (a mean rate of 0.7 hPa/hour), while the mean precipitation rate in the eyewall over six hours was around 3.7 hPa/hour – a value the authors described as “a remarkable pressure drop”.

This again implies that the convergence term was positive, and confirms that neglecting the precipitation term in the pressure tendency equation can lead to major inaccuracies.

## 2 The model of Sparks and Toumi

Without reference to prior literature on the subject, Sparks and Toumi (2022a) based their model of storm weakening on a reduced form of Eq. (2), in which the precipitation term was omitted. This same formulation was subsequently applied to the case of storm intensification (Sparks and Toumi, 2022b).

Considering a hydrostatic atmosphere

$$p = g \int_0^H \rho dz, \quad (4)$$

Sparks and Toumi (2022a, their Eq. (3)) introduced the density-weighted column-mean radial wind velocity at radius  $r$  as

$$\mathcal{U}_r \equiv \frac{\int_0^H \rho u_r dz}{\int_0^H \rho dz}. \quad (5)$$

Using Eqs. (4) and (5), Eq. (2) becomes

$$\frac{\partial \bar{p}}{\partial t} = -2p(r) \frac{\mathcal{U}_r(r)}{r} - g\bar{P}. \quad (6)$$

To derive their model for the central pressure tendency  $\partial p_c / \partial t$ , Sparks and Toumi (2022a, their Eq. (5)) neglected the last term in Eq. (6) and assumed that at the central limit  $r \rightarrow 0$  the function  $\mathcal{U}_r / r$  can be

approximated by its value (the leading term of the Taylor expansion) at the radius of maximum wind  $r_m$ , so that

$$\frac{\partial p_c}{\partial t} = -2 \lim_{r \rightarrow 0} p(r) \frac{\mathcal{U}_r(r)}{r} = -2p_c \lim_{r \rightarrow 0} \frac{\mathcal{U}_r(r)}{r} \simeq -2p_c \frac{\chi}{r_{m0}}. \quad (7)$$

Here  $\chi \equiv \mathcal{U}_r(r_{m0})$  is the column-mean radial velocity evaluated at  $r_m = r_{m0}$  at the initial point of time ( $t = 0$ ).

In the following, we demonstrate using observational data—rather than model output—that neglecting the final term in Eq. (6) is not justified, as precipitation makes a substantial contribution to the pressure tendency in both intensifying and weakening tropical cyclones.

### 3 Methods

To analyze the dependence between intensification rate and precipitation we followed the approach of Makarieva et al. (2017). We used the EBTRK dataset released on 27 July 2016 (Demuth et al., 2006) and the 3-hourly TRMM 3B42 (version 7). EBTRK data are recorded every six hours. For the years 1998–2015, for each  $k$ -th record in the EBTRK dataset (with  $(k - 1)$ th and  $(k + 1)$ th records referring to the same storm), we defined the intensification rate  $I_k \equiv -2(p_{k+1} - p_{k-1})$  (hPa day<sup>-1</sup>), where  $p$  (hPa) is the minimum central pressure. We then selected all tropical storms over land (those with a negative value of distance to land in the last column of the EBTRK file) with the known radius of maximum wind: a total of 360 values of  $I$ , of which 19 were zero, 301 negative (weakening storms) and 40 positive (intensifying storms).

Using the TRMM data (spatial resolution  $0.25^\circ$  latitude  $\times$   $0.25^\circ$  longitude), for each  $k$ -th position of the storm center in EBTRK, we established the dependence of precipitation  $P(r)$  on distance  $r$  from the storm center, with  $P(r_i)$  defined as the mean precipitation in all grid cells with  $r_i < 25i$  km,  $1 \leq i \leq 120$ ,  $r_i \equiv 25(i - 1) + 12.5$  km. Examples of  $\bar{P}(r)$  distributions for individual hurricanes are given in Fig. 11 of Makarieva et al. (2017). Maximum value of thus obtained  $\bar{P}(r_i)$  and radius  $r_i$  corresponding to this maximum were defined as  $P_m \equiv \bar{P}(r_P)$  and  $r_P$ , respectively, for the  $k$ -th record. Additionally,  $\bar{P}(r_i)$  for which  $25(i - 1) \leq r_m < 25i$  km was defined as precipitation  $\bar{P}(r_m)$  at the radius of maximum wind  $r_m$  for storms where  $r_m$  was known. To enable numerical comparison between precipitation and intensification rates<sup>1</sup>, we expressed precipitation in hPa day<sup>-1</sup> by multiplying precipitation by factor  $g$ .

<sup>1</sup>For example, one mm of water per hour (multiplied by  $\rho_l g$ , where  $\rho_l$  is the density of liquid water) is equivalent to 2.4 hPa per day.

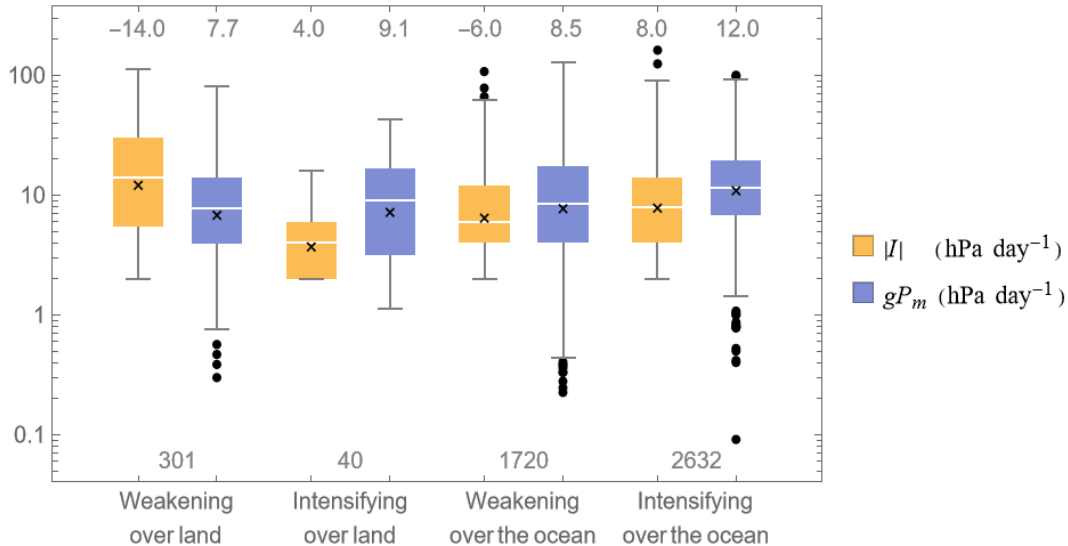


**Figure 1.** Intensification rates taken by absolute value  $|I|$  and maximum precipitation  $gP_m$  in intensifying and weakening storms on land and over the ocean (shown for comparison). Numbers of storms in each group are shown along the lower horizontal axis. Medians of  $I$  and  $gP_m$  are shown along the upper horizontal axis. Note the logarithmic scale on the vertical axis. Crosses show mean values.

#### 4 Results

The median, lower and upper quartiles for storms weakening over land are  $I = -14$  ( $-30, -5.5$ ) hPa day $^{-1}$ , while their maximum concurrent precipitation is  $gP_m = 7.7$  ( $4, 14$ ) hPa day $^{-1}$ . For storms intensifying over land  $I = 4$  ( $2, 6$ ) hPa day $^{-1}$  and  $gP_m = 9.1$  ( $3, 17$ ) hPa day $^{-1}$  (Fig. 1).

Intensification rates shown in Fig. 1 describe changes of the minimum surface pressure and thus correspond to the central pressure tendency in the axisymmetric model of Sparks and Toumi (2022a). Minimum surface pressure by definition changes faster than the mean surface pressure. Thus applying Eq. (6) to the circle  $r \leq r_P$  and neglecting the precipitation term in Eq. (6) should overestimate the absolute magnitude of  $\partial\bar{p}/\partial t$  in the weakening storms by at least  $gP_m/|I| \times 100\% \simeq 50\%$  and underestimate it in intensifying storms by  $gP_m/|I| \times 100\% = 220\%$ . For storms weakening and intensifying over the ocean, the corresponding inaccuracies would be remarkably similar at 140% and 150% (Fig. 1).

Figure 2 shows that the radius of maximum precipitation  $r_P$  is somewhat larger than the radius of maximum wind  $r_m$  that Sparks and Toumi (2022a) considered in their model, Eq. (7). Precipitation within the radius of maximum wind  $\bar{P}(r_m)$  is, by definition, lower than  $P_m$ . It was  $g\bar{P}(r_m) = 5.5$  ( $2, 11$ ) hPa day $^{-1}$  for weakening and  $g\bar{P}(r_m) = 6.2$  ( $2, 12$ ) hPa day $^{-1}$  for intensifying storms over land. The median, lower

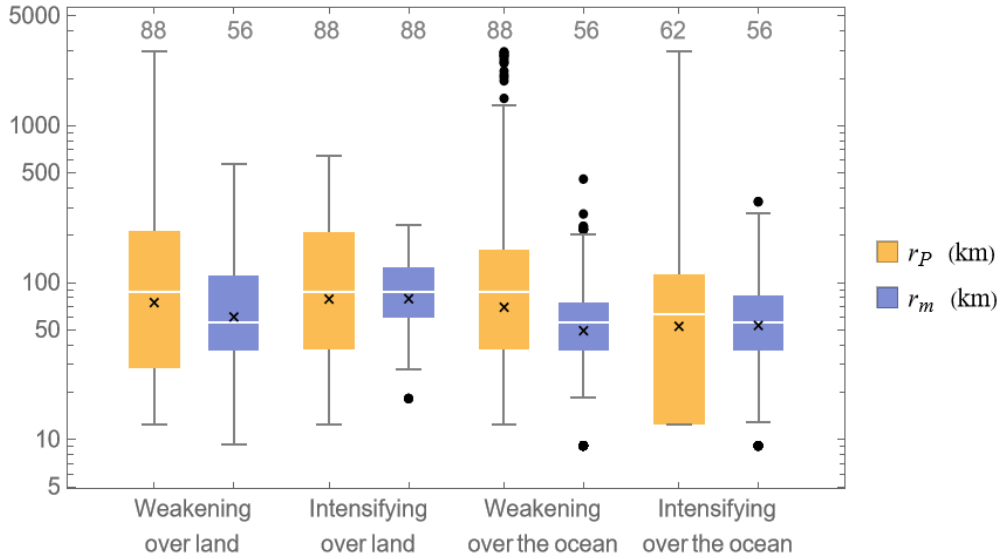


**Figure 2.** Radius of maximum precipitation  $r_P$  and radius of maximum wind  $r_m$  in storms where  $r_m$  is known. Numbers of storms in each group are the same as in Fig. 1. Medians of  $r_P$  and  $r_m$  are shown along the upper horizontal axis. Note the logarithmic scale on the vertical axis. Crosses show mean values.

and upper quartiles for the ratio  $g\bar{P}(r_m)/|I| \times 100\%$  were 40 (13, 100)% for weakening and 160 (50, 290)% for intensifying storms. This means that in both weakening and intensifying storms the vertically integrated air convergence is generally *positive*, such that the sign of the pressure tendency is decided by the absolute magnitude of precipitation rate.

Given such large inaccuracies, and under the reasonable assumption that the numerical model used by Sparks and Toumi (2022a) generated realistic precipitation, ignoring the mass sink to assess the pressure tendency from the net radial inflow alone could not produce meaningful results. Indeed, Sparks and Toumi (2022a) noted that “the density-weighted column-integrated radial wind speed”  $\mathcal{U}_r$  “was found to be unreliable when evaluated directly using instantaneous model output”, i.e., via its defining Eq. (5). Instead, to obtain reasonable agreement between their physical model and numerical simulations, Sparks and Toumi (2022a) had to resort to a circular approach – first diagnosing  $\chi$  from the mean pressure tendency using Eq. (6) (thus implicitly accounting for precipitation) and then explaining the pressure tendency using the thus-derived  $\chi$  in their model.

In other words, “column speeds”  $\mathcal{U}_r$ ,  $\chi$  and  $\chi_0$  shown in Fig. 4a,c, Fig. 6a,c and Table 1 of Sparks and Toumi (2022a) are not the actual mean column speeds but a surrogate variable  $\mathcal{U}_s$  defined from the

condition

$$-2p(r)\frac{\mathcal{U}_s(r)}{r} \equiv \frac{\partial \bar{p}}{\partial t}, \quad (8)$$

such that

$$\mathcal{U}_s \equiv \mathcal{U}_r + \frac{rg\bar{P}}{2p(r)}, \quad (9)$$

with the second term making a major contribution to the sum and of the opposite sign than the mean column speed in weakening storms. This calls for a re-consideration of the model's physical basis.

The mean column speed,  $\chi$ , as acknowledged by Sparks and Toumi (2022a), is a non-observable quantity, with its absolute magnitude being at least two orders of magnitude smaller than the actual radial velocities associated with inflow and outflow. In contrast, precipitation can be directly retrieved from observations. Sparks and Toumi (2022a) suggested that their model could be extended to tropical cyclones over the ocean. For such cases, the similarity between  $|I|$  and  $gP_m$  is even more pronounced (see Fig. 1), which led us to propose that precipitation may play a central role in both intensification and de-intensification of storms Makarieva and Nefiodov (2024). Given that precipitation is expected to increase as the radius of maximum wind contracts and vertical velocities intensify, this mechanism could explain the dependence of intensification and weakening rates on storm radius reported by Sparks and Toumi (2022b) using their model. We argue that focusing on surface pressure tendency offers a promising framework for understanding storm dynamics, provided that the role of the precipitation-induced mass sink is fully and accurately incorporated.

## 5 Pressure adjustments related to precipitation

A thought experiment can help visualize how precipitation can impact intensification. Consider a steady-state circulation with a non-condensable tracer gas (Fig. 3a). The radial inflow is equal to outflow and  $\partial \bar{p} / \partial t = 0$ . Now let us imagine that we begin to condense the tracer as it ascends, removing the condensate with precipitation (the black arrow in Fig. 3b). At the same time, we will *not* allow for any change in the flow velocity. In this imaginary case shown in Fig. 3b, the flow remains steady: there is less tracer leaving the column as gas, but this reduction of the outflow is exactly compensated by precipitation. Precipitation *per se* does not lead to either intensification or de-intensification. It just escorts the condensed vapor from the column through another exit.

However, without any flow adjustment, we would have obtained a strongly non-hydrostatic column with uncompensated vertical pressure difference  $\Delta p$  of the order of the partial pressure of water vapor  $\Delta p \sim p_v \sim 30$  hPa. Had such  $\Delta p$  persisted, we would have observed vertical velocities in excess of  $50 \text{ m s}^{-1}$ , which is clearly not the case in tropical storms. This means that precipitation *must* be accompanied by pressure adjustments. If this adjustment occurs in the vertical (Fig. 3c), the pressure deficit in the upper atmosphere will be compensated, and the outflow restored up to (maximally) its unperturbed value. With the outflow and inflow again compensating each other, the surface pressure will fall at the (maximum) rate equal to precipitation<sup>2</sup>. If the pressure adjustment occurs in the horizontal (Fig. 3d), this can lead to an additional reduction of the outflow. In this case the storm will de-intensify at a rate again (at maximum) determined by precipitation.

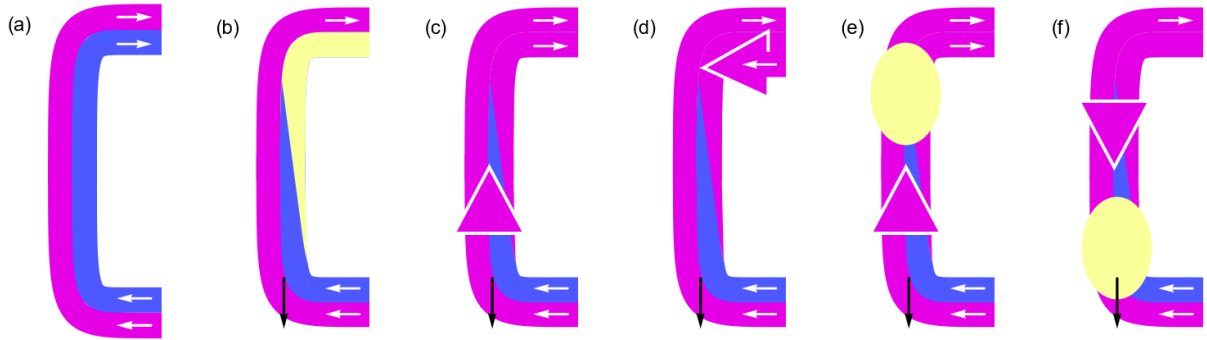


**Figure 3.** Thought experiments illustrating the role of pressure adjustments in shaping precipitation influence on storm intensification rate. Non-condensable and condensable gases are painted pink and blue, respectively. Thin white (black) arrows indicate inflow into, and outflow of gas (condensate) from, the column. Big triangles indicate the direction of pressure adjustment. Yellow spaces indicate pressure perturbations.

Another way to look at the pressure adjustment problem is as follows. Is it possible to remove condensate from the atmosphere without disturbing the hydrostatic equilibrium? Consider again a hydrostatic column, where condensation and precipitation take place. At height  $z$  we have

$$-\frac{\partial p}{\partial z} = \rho g = \frac{p}{h}, \quad h \equiv \frac{RT}{Mg}, \quad (10)$$

<sup>2</sup>For example, Hurricane Milton 2024 that underwent rapid intensification at  $84 \text{ hPa day}^{-1}$ , should have had a precipitation maximum of at least  $35 \text{ mm hour}^{-1}$ . Reconnaissance flights into Milton recorded maximum local precipitation in excess of  $30 \text{ mm hour}^{-1}$  and up to over  $60 \text{ mm hour}^{-1}$ , see <https://tropicalatlantic.com/recon/recon.cgi?basin=al&year=2024&product=hdob&storm=Milton&mission=16&agency=AF&ob=10-09-010230-38-910.3-140-164>.

where  $R$  is the universal molar gas constant, and the ideal gas equation of state  $p = (\rho/M)RT$  is taken into account. For simplicity we ignore the difference in the molar masses  $M$  of water vapor and dry air. Assuming air convergence to be negligible, the continuity equation reads

$$\frac{\partial \rho}{\partial t} = \dot{\rho}. \quad (11)$$

Assuming also that temperature  $T$  does not change, the rate of pressure fall is determined solely by the condensation rate, i.e., by the pressure sink  $\dot{p}$  ( $\text{W m}^{-3}$ ):

$$\frac{\partial p}{\partial t} \simeq \frac{RT}{M} \frac{\partial \rho}{\partial t} = gh\dot{\rho} \equiv \dot{p} < 0. \quad (12)$$

Differentiating Eq. (10) with respect to time and taking into account Eq. (12), we obtain

$$\frac{\partial \ln \dot{p}}{\partial z} = \frac{\partial \ln p}{\partial z} = -\frac{1}{h}. \quad (13)$$

This means that the removal of condensate from the atmospheric column will not disturb the hydrostatic equilibrium if the pressure sink is proportional to pressure itself, i.e., if  $\dot{p}(z) = kp(z)$ , where  $k$  is independent of altitude  $z$ .

In the real atmosphere, condensation rate  $\dot{\rho}$  is known to be determined by the material derivative of the water vapor mixing ratio (e.g., Bryan and Rotunno, 2009, their Eq. (6)), to which the product of the vertical velocity and the vertical gradient of the water vapor mixing ratio makes a major contribution. Accordingly, the (steady-state) pressure sink  $\dot{p}$  is approximately given by  $\dot{p} = wp\partial\gamma/\partial z$  (e.g., Gorshkov et al., 2012, their Eq. (18)), such that  $k = w\partial\gamma/\partial z$ , where  $\gamma \equiv p_v/p$  is the ratio of water vapor partial pressure  $p_v$  to total pressure  $p$ . There are no grounds to expect the function  $w\partial\gamma/\partial z$  to generally be a constant with respect to  $z$ . While at higher temperatures  $\partial\gamma/\partial z$  can be approximately constant below  $z \lesssim 10$  km as governed by moist thermodynamics (e.g., Makarieva et al., 2013, their Fig. 2), the vertical velocity  $w$  can in principle change arbitrarily over  $z$ .

If  $k(z)$  has a maximum, and condensation is predominantly concentrated, in the upper atmosphere (Fig. 3e), then the pressure adjustment will be predominantly directed upward leading to intensification (could convective bursts preceding rapid intensification be an example?) If, on the contrary,  $k(z)$  is maximized, and condensation more intense, in the lower atmosphere, then the pressure adjustment will proceed downward suppressing the upwelling and possibly resulting in de-intensification (Fig. 3f). The intensification rate can become zero, and the storm steady, at some intermediate position of the conden-

sation maximum<sup>3</sup>. In the view of  $|I| \simeq gP$ , the concepts shown in Fig. 3 are clearly relevant to storm intensification, but largely remain unstudied.

If, as indicated by the data in Fig. 1, the vertically integrated air convergence is usually positive, and the negative sign of the pressure tendency in the intensifying storms is ensured by precipitation, it is clear that relatively minor changes in precipitation can turn a strengthening storm into a weakening one. This pattern was observed by Su et al. (2020) who found that in all intensity categories, from tropical depressions to intense hurricanes, intensifying storms differ from weakening ones by a nearly universal precipitation surplus of 2 mm/hour in the storm core. Smith et al. (2021) observed, in a modeling study, that the appearance of a low-level outflow is associated with storm weakening. This is also understandable in terms of the precipitation impact: unlike a high-level outflow, a low-level one does not generate much precipitation. So as soon as the air ceases to ascend, precipitation drops and the storm begins to weaken.

We argue that focusing on surface pressure tendency offers a promising framework for understanding storm intensification and weakening, provided that the role of the precipitation-induced mass sink is fully and accurately incorporated.

## Acknowledgments

Work of A.M. Makarieva is partially funded by the Federal Ministry of Education and Research (BMBF) and the Free State of Bavaria under the Excellence Strategy of the Federal Government and the Länder, as well as by the Technical University of Munich – Institute for Advanced Study.

## Datastatement

The raw data utilised in this study were derived from the following resources available in the public domain: [https://disc.gsfc.nasa.gov/datasets/TRMM\\_3B42\\_7/summary](https://disc.gsfc.nasa.gov/datasets/TRMM_3B42_7/summary) and [https://rammb2.cira.colostate.edu/research/tropical-cyclones/tc\\_extended\\_best\\_track\\_dataset/](https://rammb2.cira.colostate.edu/research/tropical-cyclones/tc_extended_best_track_dataset/).

---

<sup>3</sup>With vertical velocity freely varying along height, these conclusions do not depend on our neglect of the difference in the molar masses of water vapor and dry air made when deriving Eq. (13). Whatever the exact form of Eq. (13), it does not contain vertical velocity.

## References

- Bryan, G. H. and Rotunno, R.: The maximum intensity of tropical cyclones in axisymmetric numerical model simulations, *Mon. Wea. Rev.*, 137, 1770–1789, <https://doi.org/10.1175/2008MWR2709.1>, 2009.
- Demuth, J. L., DeMaria, M., and Knaff, J. A.: Improvement of advanced microwave sounding unit tropical cyclone intensity and size estimation algorithms, *J. Appl. Meteor. Climatol.*, 45, 1573–1581, <https://doi.org/10.1175/JAM2429.1>, 2006.
- Gorshkov, V. G., Makarieva, A. M., and Nefiodov, A. V.: Condensation of water vapor in the gravitational field, *J. Exp. Theor. Phys.*, 115, 723–728, <https://doi.org/10.1134/S106377611209004X>, 2012.
- Lackmann, G. M. and Yablonsky, R. M.: The importance of the precipitation mass sink in tropical cyclones and other heavily precipitating systems, *J. Atmos. Sci.*, 61, 1674–1692, [https://doi.org/10.1175/1520-0469\(2004\)061<1674:TIOTPM>2.0.CO;2](https://doi.org/10.1175/1520-0469(2004)061<1674:TIOTPM>2.0.CO;2), 2004.
- Makarieva, A. M. and Nefiodov, A. V.: Condensation mass sink and intensification of tropical storms, <https://arxiv.org/abs/2401.16331v1>, eprint arXiv: 2401.16331v1 [physics.ao-ph], 2024.
- Makarieva, A. M., Gorshkov, V. G., Nefiodov, A. V., Sheil, D., Nobre, A. D., Bunyard, P., and Li, B.-L.: The key physical parameters governing frictional dissipation in a precipitating atmosphere, *J. Atmos. Sci.*, 70, 2916–2929, <https://doi.org/10.1175/JAS-D-12-0231.1>, 2013.
- Makarieva, A. M., Gorshkov, V. G., Nefiodov, A. V., Chikunov, A. V., Sheil, D., Nobre, A. D., and Li, B.-L.: Fuel for cyclones: The water vapor budget of a hurricane as dependent on its movement, *Atmos. Res.*, 193, 216–230, <https://doi.org/10.1016/j.atmosres.2017.04.006>, 2017.
- Montgomery, M. T. and Smith, R. K.: Recent developments in the fluid dynamics of tropical cyclones, *Annu. Rev. Fluid Mech.*, 49, 541–574, <https://doi.org/10.1146/annurev-fluid-010816-060022>, 2017.
- Smith, R. K., Kilroy, G., and Montgomery, M. T.: Tropical cyclone life cycle in a three-dimensional numerical simulation, *Quart. J. Roy. Meteor. Soc.*, 147, 3373–3393, <https://doi.org/10.1002/qj.4133>, 2021.
- Sparks, N. and Toumi, R.: A physical model of tropical cyclone central pressure filling at landfall, *J. Atmos. Sci.*, 79, 2585–2599, <https://doi.org/10.1175/JAS-D-21-0196.1>, 2022a.
- Sparks, N. and Toumi, R.: The dependence of tropical cyclone pressure tendency on size, *Geophys. Res. Lett.*, 49, e2022GL098926, <https://doi.org/10.1029/2022GL098926>, 2022b.
- Su, H., Longtao, W., Jiang, J. H., Pai, R., Liu, A., Zhai, A. J., Tavallali, P., and DeMaria, M.: Applying satellite observations of tropical cyclone internal structures to rapid intensification forecast with machine learning, *GRL*, 47, e2020GL089102, <https://doi.org/10.1029/2020GL089102>, 2020.
- Trenberth, K. E.: Climate diagnostics from global analyses: Conservation of mass in ECMWF analyses, *J. Climate*, 4, 707–722, [https://doi.org/10.1175/1520-0442\(1991\)004<0707:CDGAC>2.0.CO;2](https://doi.org/10.1175/1520-0442(1991)004<0707:CDGAC>2.0.CO;2), 1991.
- Wacker, U., Frisius, T., and Herbert, F.: Evaporation and precipitation surface effects in local mass continuity laws of moist air, *J. Atmos. Sci.*, 63, 2642–2652, <https://doi.org/10.1175/JAS3754.1>, 2006.